An Oligodendrocyte Cell Adhesion Molecule at the Site of Assembly of the Paranodal Axo-Glial Junction

Steven Tait,* Frank Gunn-Moore,* J. Martin Collinson,* Jeffery Huang‡ Catherine Lubetzki,§ Liliana Pedraza,‡ Diane L. Sherman,* David R. Colman,‡ and Peter J. Brophy*

*Department of Preclinical Veterinary Sciences, University of Edinburgh, Edinburgh EH9 1QH, United Kingdom; ‡Department of Biochemistry and Molecular Biology, Program in Cell Adhesion, Mount Sinai School of Medicine, New York, New York 10029; and §INSERM U-495, Biologie des Interactions Neurones/Glie, Hôpital de la Salpetrière, 75651 Paris Cedex 13, France

Abstract. Two major isoforms of the cell adhesion molecule neurofascin NF186 and NF155 are expressed in the central nervous system (CNS). We have investigated their roles in the assembly of the node of Ranvier and show that they are targeted to distinct domains at the node. At the onset of myelination, NF186 is restricted to neurons, whereas NF155 localizes to oligodendrocytes, the myelin-forming glia of the CNS. Coincident with axon ensheathment, NF155 clusters at the paranodal regions of the myelin sheath where it localizes in apposition to the axonal adhesion molecule paranodin/contactin-associated protein (Caspr1), which is a constituent of the septate junction-like axo-glial adhesion zone. Immunoelectron microscopy confirmed that neurofascin is a glial component of the paranodal axo-glial junction. Concentration of NF155 with Caspr1 at the paranodal junctions of peripheral nerves is also a feature of Schwann cells. In *Shiverer* mutant mice, which assemble neither compact CNS myelin nor normal paranodes, NF155 (though largely retained at the cell body) is also distributed at ectopic sites along axons, where it colocalizes with Caspr1. Hence, NF155 is the first glial cell adhesion molecule to be identified in the paranodal axo-glial junction, where it likely interacts with axonal proteins in close association with Caspr1.

Key words: glia • node of Ranvier • neurofascin • myelination • paranode

Introduction

The rapid rate of nerve impulse conduction, which is characteristic of myelinated fibers in the central nervous system (CNS),[1] is dependent on the high density of sodium channels at the node of Ranvier (Ritchie and Rogart, 1977). Therefore, clustering of these ion channels is a key event in the morphological and functional maturation of the vertebrate CNS. Oligodendrocytes, the myelin-forming glia of the CNS, are believed to have an important role in sodium channel clustering (Vabnick and Shrager, 1998). One proposal is that oligodendrocytes exert their influence on neurons by means of a secreted factor (Kaplan et al., 1997). More recent work has highlighted the significance of axo-glial contact adjacent to the node as a prerequisite for the assembly of a functional node (Rasband et al., 1999). These paranodal axo-glial adhesive zones bear a strong morphological similarity to the septate junctions found in invertebrates (for review see Salzer, 1997).

In addition to their putative involvement in defining the site of the node of Ranvier, paranodal axo-glial junctions are also believed to function as a barrier to ion flow in the mature nerve (Chiu and Ritchie, 1981). However, in spite of their probable importance, the molecular basis of axo-glial interaction at the paranodal junctions is still poorly understood. Paranodin/Caspr1 (contactin-associated protein 1) is an axonal constituent of the axo-glial adhesion zone and has been proposed to play an important role in paranodal junction formation (Einheber et al., 1997; Menegoz et al., 1997; Peles et al., 1997a,b). Support for this view has come from studies on the nerves of *Shiverer* (*Shi*) mouse mutants and of mice deficient in the enzyme UDP-galactose-ceramide galactosyltransferase (CGT) in which Caspr1 fails to concentrate at the paranodes (Dupree et al., 1999; Rasband et al., 1999). How-

Address correspondence to Dr. Peter J. Brophy, Department of Preclinical Veterinary Sciences, University of Edinburgh, Summerhall, Edinburgh EH9 1QH, UK. Tel.: 44-131-650-6107. Fax: 44-131-650-6576. E-mail: peter.brophy@ed.ac.uk

[1]*Abbreviations used in this paper:* Caspr, contactin-associated protein; CNS, central nervous system; DRG, dorsal root ganglion; FNIII, fibronectin type III; MAG, myelin-associated glycoprotein; PNS, peripheral nervous system; RT, reverse transcriptase.

ever, the glial counterparts of Caspr1 have yet to be identified.

Neurofascin is an ankyrin-binding, cell adhesion molecule of the L1 subgroup of the immunoglobulin G superfamily that has been implicated in neurite outgrowth, fasciculation, and interneuronal adhesion (Rathjen and Schachner, 1984; Grumet et al., 1991; Volkmer and Rathjen, 1992; Volkmer et al., 1992; Davis et al., 1993; Zhang et al., 1998). The neurofascin gene is subject to extensive alternative splicing (Hassel et al., 1997), and two of the best characterized products are a 186-kD isoform (NF186), typical of myelinated axons, and found at nodes of Ranvier and axonal initial segments, and a 155-kD isoform (NF155), which has been localized to unmyelinated axons in the peripheral nervous system (PNS; Davis et al., 1996). Compared with NF 186, NF155 contains an extra fibronectin type III (FNIII) repeat and lacks a mucinlike domain (Davis et al., 1996).

All functional studies of neurofascin have sought to elucidate its role in neurons (Rathjen and Schachner, 1984; Rathjen et al., 1987a,b; Brummendorf and Rathjen, 1996; Brummendorf et al., 1998). However, there is some evidence that neurofascin might be expressed in cells that have been identified, on the basis of their morphology, as oligodendrocytes (Moscoso and Sanes, 1995). We have confirmed this observation and have suggested that the specific isoform expressed in oligodendrocytes is NF155 (Collinson et al., 1998). Expression of neurofascin mRNA is first detectable at the initiation of myelination, but once the ensheathment of target axons begins in earnest, the amount of neurofascin mRNA in oligodendrocytes declines precipitously. This transient peak of expression at the onset of myelination in the CNS suggested that neurofascin might be a strong candidate to mediate and signal axon–glial interaction. Here, we show that NF155 is targeted to the paranodal loops of the sheath, where they interact with Caspr1 on the axon. Hence, NF155 is the first glial cell adhesion molecule of the paranodal junctional complex to be described.

Materials and Methods

Antibodies, Immunoprecipitation, and Immunoblotting

Antibodies against neurofascin were generated in New Zealand white rabbits against three peptides coupled to keyhole Limpet hemocyanin by means of a terminal cysteine (Research Genetics). The first antibody (NFC1) was raised against a region at the extreme COOH terminus of the intracellular domain common to both NF186 and NF155 (CGNESSEATSPVNAAIYSLA), the second (NFF3) to the third FNIII domain specific to NF155 (CLWVSQKRQQASFPGDRPR), and the third (MNF2) to a sequence within the mucin domain specific to NF186 (CTESPTTTTGTKIHETAPDEQS).

Each antibody was affinity-purified by immunoabsorption to a column of peptide coupled to aminohexyl Sepharose 4B (Sigma Chemical Co.). Other primary antibodies used were against myelin-associated glycoprotein (MAG; mouse mAb; Boehringer Mannheim), ankyrin$_G$ (mouse monoclonal; Zymed Laboratories Inc.), phosphorylated neurofilament M NFM (mouse monoclonal, RMO108; a gift of Dr. V.M.-Y. Lee, University of Pennsylvania, Philadelphia, PA) contactin (rabbit antiserum, a gift from Dr. J. Trotter, Department of Neurobiology, University of Heidelberg, Germany), and phosphotyrosine (mouse monoclonal MCPY; Upstate Biotechnology). The cDNA of the entire Caspr1 cytoplasmic region was used to generate rabbit and guinea pig antisera, as has been described elsewhere (Menegoz et al., 1997; Peles et al., 1997b). In brief, the primers that flank the cytoplasmic region were used in reverse transcriptase (RT)–PCR of RNA from adult rat brain stem and cerebellum. The resulting cDNA was cloned into pGEX4T2 (Amersham Pharmacia Biotech) and verified by sequencing. The fusion protein expressed in *Escherichia coli* (strain BL21; Stratagene) was purified on glutathione-Sepharose (Amersham Pharmacia Biotech).

Peroxidase-coupled antisera were purchased from the Scottish Antibody Production Unit. Antisera and affinity-purified antibodies (NFC1, 1:2,000; NFF3, 1:100; and MNF2, 1:100) were tested by Western blot analysis as described previously (Gillespie et al., 1994). For immunoprecipitation, optic nerves or brains were removed from 10- and 12-d-old mice and homogenized in 250 μl ice-cold lysis buffer (25 mM Hepes, 10 mM EDTA, 5 mM NaF, 15 mM $Na_4P_2O_7 \cdot 10\ H_2O$, 1 mM benzamidine, 0.5 mM Na_3VO_4, peptide inhibitors [P8340; Sigma Chemical Co.], and 1 mM PMSF, pH 7.4). The homogenate was solubilized for 5 min on ice by adding an equal volume of 2% Triton X-100 in lysis buffer. After centrifugation at 4°C for 15 min at 13,000 *g*, NFC1 or Caspr1 antibody at a dilution of 1:100 coupled to 5 mg of protein A agarose was added to the cleared supernatant and tumbled for 2 h at 4°C. The immune complexes were harvested by centrifugation and washed twice with lysis buffer and twice with 0.1% Triton X-100 in lysis buffer. Proteins were solubilized, resolved on 8% SDS polyacrylamide gels, and transferred electrophoretically to Protran nitrocellulose (Schleicher & Schuell) as previously described (Gillespie et al., 1994). The membrane was blocked overnight in 5% milk solids and probed with NFC1 (1:2,000), anti-Caspr1 (1:1,000), or anticontactin (1:1000) diluted in PBS containing 0.2% gelatin, 0.1% Tween 20, pH 7.4; followed by goat anti–rabbit IgG-HRP conjugate (1:1,000), or with MCPY diluted (1:1,000) in 3% milk solids in PBS, followed by goat anti–mouse IgG-HRP conjugate (1:2,000). Conjugates were detected using the ECL system according to the manufacturer's instructions (Amersham International).

Cell Cultures

Dorsal root ganglion (DRG) cultures were prepared following the procedure described by Bunge and co-workers (Kleitman et al., 1991). In brief, 12-mm glass coverslips, inserted into 4-well dishes (NUNC), were coated at room temperature for 1 h with Matrigel (Collaborative Biomedical products) diluted 1:30 in L15 medium. Spinal cords were removed from E16 Sprague-Dawley rat embryos, and the attached DRGs were removed and dissociated by trypsin treatment before plating on the matrigel-coated coverslips. Dissociated DRG were plated in C media (MEM, 10% FCS, 0.4% glucose, and 100 ng/ml NGF). After two cycles of antimitotic feeding (Kleitman et al., 1991), the cultures were reseeded with Schwann cells. Ascorbic acid (50 μg/ml) was added to the medium to trigger myelination. Primary Schwann cells were prepared from newborn rat sciatic nerves following the method described by Brockes (Brockes et al., 1979). Schwann cells were grown on poly-L-lysine–coated coverslips in DME containing 10% FCS.

Immunofluorescence Microscopy

CNS and PNS tissues were fixed by transcardial perfusion with 4% paraformaldehyde in 0.1 M sodium phosphate, pH 7.4. After extensive washing with 0.1 M sodium phosphate, pH 7.4, the tissue was cryoprotected by immersion for 15 min each in 5%, then 10% sucrose in 0.1 M phosphate buffer, pH 7.4, and finally overnight in 25% sucrose in 0.1 M phosphate buffer, pH 7.4, at 4°C. After embedding in OCT (Tissue TEK) blocks were frozen in isopentane cooled in liquid nitrogen. Sections (8–10 μm) were collected on 3-aminopropyltriethoxysilane subbed glass slides, and OCT was removed by washing in PBS (Sigma Chemical Co.). Sciatic nerve fibers were teased in 0.1% Triton X-100 in PBS. Before incubation with the NFF3 antibody, sections or teased sciatic nerve fibers were treated with Bouin's reagent for 1 min. Samples were blocked for 3 h in 0.2% Triton X-100, 0.2% gelatin in PBS, pH 7.4, containing either 10% nonimmune goat serum when using rabbit and mouse primary antibodies, or donkey serum when the sheep antibody was used. The antibodies were applied overnight in 4% nonimmune serum in the same buffer, and after washing them in buffer without serum, fluorescently labeled secondary antibodies were applied for 2 h in buffer containing serum, followed by further washes. Secondary antibodies were as follows: FITC-labeled goat anti–rabbit (Cappel Laboratories), TRITC-labeled goat anti–mouse IgG_1, TRITC-labeled donkey anti–rabbit (Jackson Laboratories), and FITC-labeled donkey anti–sheep (Jackson Laboratories). Further washes in blocking buffer minus serum were followed by several washes in PBS. Sections were mounted in Vectashield (Vector Laboratories). Images were captured with a Leica TCS4D confocal or Olympus BX60 microscope, and figures were produced with Adobe Photoshop.

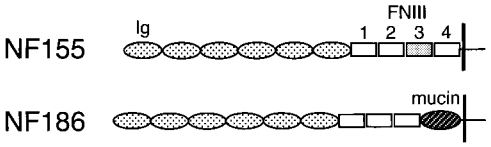

Figure 1. Domain structure of NF186 and NF155 showing the mucin domain and the third fibronectin type III repeat unique to the two respective isoforms (Davis et al., 1996).

Immunoelectron Microscopy

Mice were perfused transcardially with heparinized (200 U heparin/100 ml) saline (0.89% NaCl) followed by freshly prepared 4% paraformaldehyde, 0.1% glutaraldehyde in 0.1 M sodium phosphate buffer, pH 7.4 for 2 h. The tissue was washed several times with 0.1 M sodium phosphate buffer, pH 7.4, containing 3.5% sucrose and stained with 0.25% tannic acid in the same buffer for 1 h at 4°C (subsequent steps were performed at 4°C). Aldehydes were quenched with 50 mM NH_4Cl in 0.1 M sodium phosphate buffer, pH 7.4. The tissue was washed four times in 0.1 M maleate buffer, pH 6.2, containing 4% sucrose, followed by 1% uranyl acetate in the maleate sucrose buffer for 1 h. The tissue was dehydrated to 100% ethanol (from 70% ethanol onward all steps were at −20°C), infiltrated with a 1:1 ratio of LR Gold (Agar Scientific Ltd.) and ethanol, followed by a 7:3 ratio of LR Gold and ethanol, and two changes of LR Gold for 2–3 h each. The tissue was infiltrated overnight in LR Gold containing 0.5% benzoin methyl ether and embedded in gelatin capsules. Polymerization was by UV irradiation at a wavelength of 365 nm for 24 h at −20°C.

Sections on formvar carbon–coated nickel grids were blocked for 40 min at room temperature with 1% BSA, 0.5% fish skin gelatin, 0.05% Triton X-100, 0.05% Tween 20 in 10 mM Tris buffer, pH 7.4, containing 500 mM NaCl, and incubated with NFC1 antibody in the same buffer at 4°C overnight. Grids were washed four times with the above buffer and incubated for 1 h with goat anti–rabbit IgG conjugated to 10 nm gold (1:20 Avrion). The grids were washed on drops of distilled water, fixed with 2.5% aqueous glutaraldehyde, and rinsed in a stream of distilled water. After postfixing for 15 min with 2% aqueous OsO_4, the grids were stained with uranyl acetate and lead citrate and examined at 80 kV in a Phillips Biotwin electron microscope.

In Situ Hybridization

RNA was prepared from adult mouse brains by TRIZOL extraction (Life Technologies) for RT-PCR. Reverse transcription was performed with 1 μg of RNA using SuperScript™II reverse transcriptase (400 U; Life Technologies) in the presence of random hexamers (Life Technologies). After incubation at 42°C for 45 min, reactions were terminated by heating at 80°C. DNA in 1 μl of the first strand reaction was amplified by PCR with Dynazyme (Flowgen). Primer sequences were selected from the published neurofascin (ankyrin-binding protein) sequence (available from GenBank/EMBL/DDBJ under accession No. L11002) (Davis et al., 1996) that would specifically amplify products from either the 155- or 186-kD splice variants of neurofascin (see Fig. 1). A probe specific for NF155 was amplified from within the third FNIII domain of neurofascin with a forward primer, 5′-CCTGAACAGCACAGCCATCAG-3′ (nucleotides 3,550–3,570) and a reverse primer 5′-GACCACAACCATCTCCTGCTTG-3′ (nucleotides 3,775–3,754). A probe specific for NF186 was amplified from within the mucin domain of neurofascin using a forward primer, 5′-TGTGAGCAGTACTGATGCTAC-3′ (nucleotides 4,189–4,209) and a reverse primer, 5′-GTGATGACGGTACTGCTGAATG-3′ (nucleotides 4,635–4,615). The products were cloned into the pGEM-T vector (Promega) and sequenced. The cDNA templates were linearized with either NotI or NcoI and transcribed with either T7 (antisense probes) or SP6 RNA (sense probes) polymerases (Boehringer Mannheim), respectively. The cRNA probes were labeled with [^{35}S]UTP and hybridized to sections (5–10 μm) of fresh mouse tissue that had been frozen in isopentane cooled to −70°C on liquid nitrogen as described (Collinson et al., 1998).

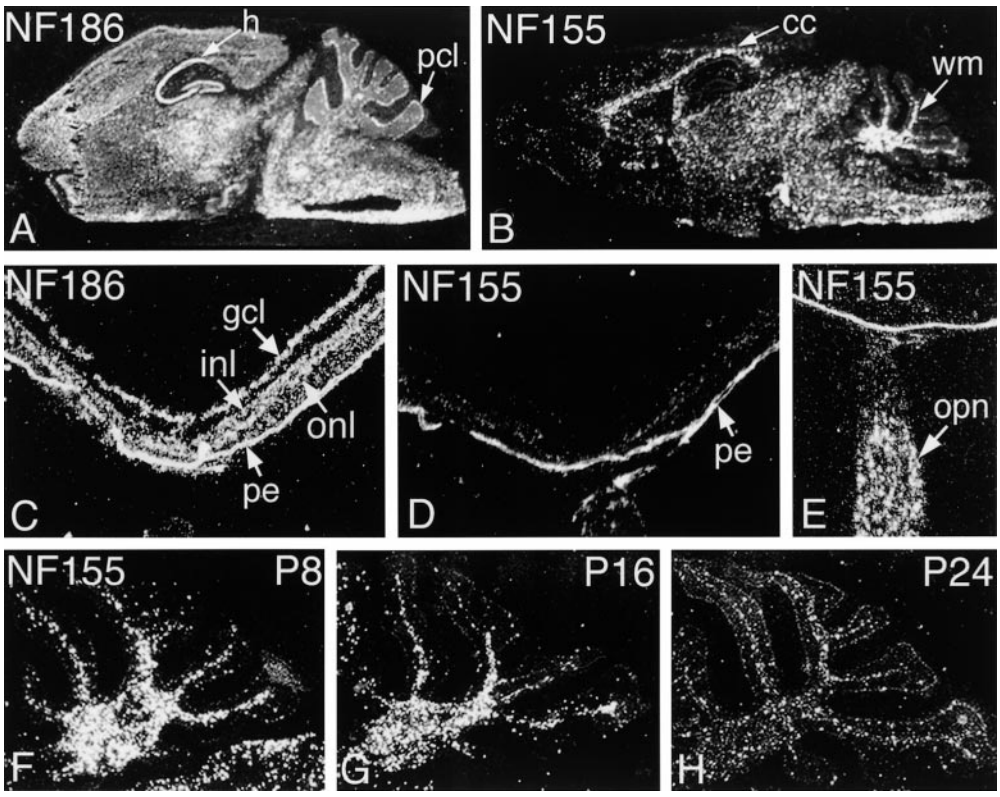

Figure 2. Differential expression of NF186 and NF155 transcripts in mouse CNS. Mouse parasagittal brain sections (A and B) retinas (C and D), optic nerve, and parasagittal sections of cerebellum at different postnatal ages (F–H) were hybridized with riboprobes specific for NF186 (A and C) or NF155 (B and D–H) and viewed by dark-field microscopy. NF186 signal was disseminated, but clearly recognizable in certain neuronal populations such as in the hippocampus (h) and the cerebellar Purkinje cell layer (A, pcl). NF155 transcripts were concentrated in the oligodendrocyte- and myelin-rich corpus callosum (cc) and cerebellar white matter (wm) tracts (B). Neurons in the retinal ganglion cell layer (gcl), inner nuclear layer (inl), or outer nuclear layer (onl) bodies were rich in NF186 transcripts (C) but were devoid of NF155 mRNA (D). Note that the retinal pigment epithelium layer (pe) appears as a bright line in dark-field microscopy (C–E). Robust expression of NF155 mRNA in cells that were presumed to be oligodendrocytes was found in the optic nerve at P12 (E). NF155 mRNA levels declined from P8 at the early stages of myelination to P24 (F–H) in the cerebellar white matter although expression persisted in these tracts at a low level (H).

Results

NF186 and NF155 Are Differentially Expressed in Neurons and Glia

Neurofascin has been characterized as a neuronal cell adhesion molecule in the developing and mature CNS (Rathjen et al., 1987a,b; Davis et al., 1996). However, we also demonstrated strong expression of the gene by in situ hybridization in oligodendrocytes (Collinson et al., 1998). Furthermore, it appeared that in the myelinating optic nerve, which does not contain neuronal mRNAs, the primary neurofascin transcript appeared to be NF155 rather than NF186 (Collinson et al., 1998). To establish if these two neurofascin isoforms were indeed expressed in a cell type–specific fashion in the CNS, we prepared probes for in situ hybridization and for immunocytochemistry that recognized the mucin (NF186) or the third fibronectin type III (NF155) domains (Fig. 1). In situ hybridization analysis of postnatal day 21 (P21) mouse brain with isoform-specific riboprobes demonstrated that NF186 mRNA was widely distributed with strong signals from certain neuron populations such as the hippocampus and the Purkinje cells of the cerebellum (Fig. 2 A). In contrast, NF155 mRNA was strongly expressed in white matter tracts (Fig. 2 B).

The differential expression of the two neurofascin isoforms was seen most dramatically in the retina and optic nerve. The neurons of the retina, including the ganglion cells, which project their axons to the optic nerve, were devoid of NF155 mRNA (Fig. 2 D), whereas each of the retinal neuron layers displayed strong signals with the NF186 probe (Fig. 2 C). In contrast, cells in the optic nerve itself, which were presumed to be oligodendrocytes, were strongly labeled with the NF155-specific riboprobe (Fig. 2 E). The use of a specific riboprobe confirmed the transient nature of NF155 expression during the most active period of myelination in the cerebellar white matter tracts that had been observed earlier with a nonspecific neurofascin probe (Fig. 2, F–H; Collinson et al., 1998). We found that,

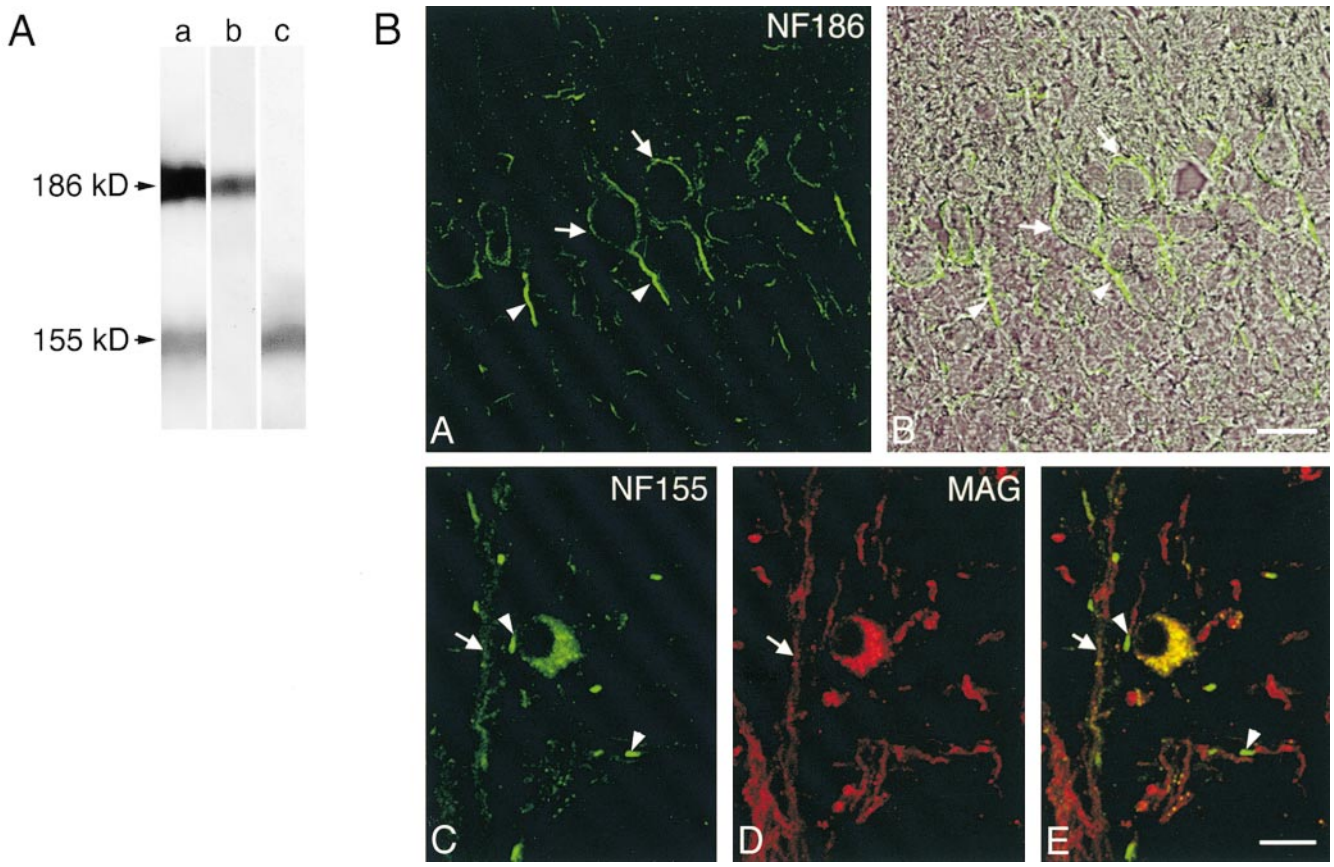

Figure 3. (A) Characterization of neurofascin isoform-specific antibodies. Three rabbit antibodies were tested by Western blotting using mouse optic nerve homogenate. The first antibody (NFC1) was raised against a region at the extreme COOH terminus of the intracellular domain common to both NF186 and NF155 (lane a), the second (MNF2) to a sequence within the mucin domain specific to NF186 (lane b) and the third (NFF3) to the third FNIII domain specific to NF155 (lane c). (B) Immunolocalization of NF186 and NF155 to neurons and oligodendrocytes, respectively. Purkinje cell neurons of the cerebellum are strongly positive for NF186, particularly in the plasma membrane (arrows) and initial axonal segment (arrowheads) (A, fluorescence; B, fluorescence with phase overlay). A striatal oligodendrocyte is shown labeled with antibodies against NF155 (C) and MAG (D), an oligodendrocyte marker. The overlay (E) shows that the two proteins colocalize to the oligodendrocyte cell body and the early wraps of myelin around the axon (arrow). In addition, punctate staining with the anti-NF155 antibody can be observed at sites that are presumed to be nascent paranodes (arrowheads, and see Fig. 4). Bars, 10 μm.

in a similar fashion, the expression of NF155 transcripts in the developing optic nerve also declined after a transient peak of expression (data not shown). All sense riboprobe controls yielded no discernible signal (data not shown).

To demonstrate that these cells were indeed oligodendrocytes, we generated neurofascin isoform–specific antibodies (Fig. 3 A). In optic nerve extracts, neither of these antibodies detected the minor 140-kD isoform of neurofascin found in other regions of the brain (Davis et al., 1996). NF186 protein was clearly neuronal, as demonstrated by strong expression in the plasma membrane and initial segments of the Purkinje cells of the cerebellum (Fig. 3 B, A and B) as previously shown by Bennett and co-workers (Davis et al., 1996). Double labeling for NF155 and an antibody against the oligodendrocyte marker MAG demonstrated that, at early stages of myelination, neurofascin was expressed in the cell bodies of oligodendrocytes (Fig. 3 B, C–E). Some punctate staining for NF155 was also observed which probably represented nascent paranodal labeling (see below). The NF155 antibody was shown to be specific for myelinating oligodendrocytes because, at the onset of myelination, those cell bodies detected by the NF155 antibody were always MAG-positive. This excludes expression of NF155 by astrocytes or oligodendrocyte precursors in the optic nerve.

NF155 Localizes to the Paranodal Axo-Glial Junction

In the myelinating optic nerve, NF155 is first observed at the cell body of the oligodendrocyte and in a diffuse pattern on the first processes of the myelin sheath as they engage the axon (Fig. 4 A, A and B). A dramatic restriction in the localization of the protein occurs over the next two days: the protein is no longer detectable in oligodendrocyte cell bodies, but it is concentrated in puncta on nerve fibers (Fig. 4 A, C and D). These foci of expression correspond to paranodes since they flank the nodes of Ranvier, at which ankyrin$_G$ is concentrated in myelinated nerves (Fig. 4 B, A–C; Kordeli et al., 1995). In contrast, NF186 colocalizes with ankyrin$_G$, confirming its association with the axonal membrane at the node of Ranvier (Davis et al., 1996). Evidence that NF155 is a glial component of the paranodal axo-glial junction was provided by immunoelectron microscopy. In a longitudinal section (Fig. 5, A, A′, B, and C) and in a tangential section (Fig. 5 D), the protein is seen to be localized at the base of the cytoplasm-filled paranodal loops, where they appose the axonal membrane. Although tyrosine phosphorylation inhibits the ankyrin-mediated association of neurofascin with the actin cytoskeleton (Tuvia et al., 1997), restriction of NF155 to paranodes in the optic nerve does not appear to require complete dephosphorylation since NF155 is phosphory-

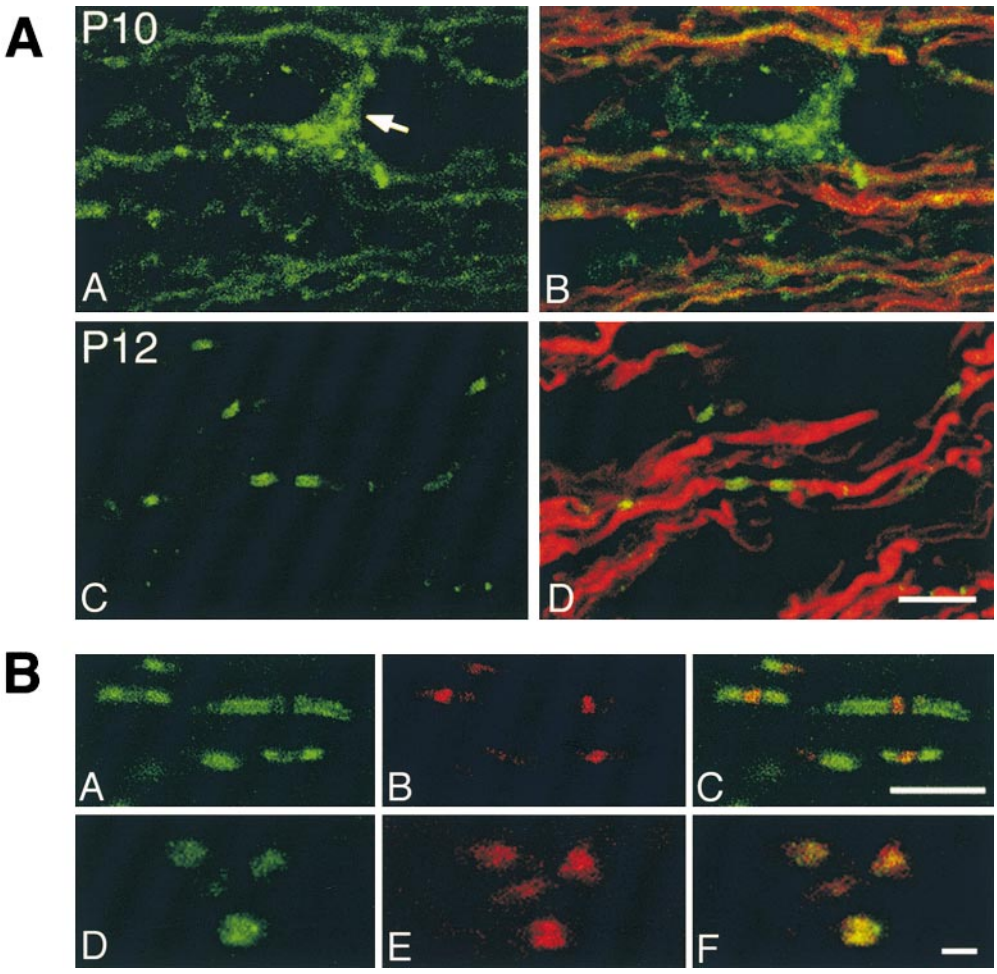

Figure 4. In the nodal region, NF155 is concentrated at the paranodes of myelinated fibers in the mouse optic nerve, whereas NF186 is restricted to the node of Ranvier. (A) NF155 (green) either alone (A and C) or overlaid with NF-M neurofilament staining (red, B and D) displayed a dramatic restriction in localization between P10 and P12 in the optic nerve. (B) Double labeling with an antibody that recognizes both NF155 and NF186 (A) or NF186 (D) with an antibody that identifies the node of Ranvier marker ankyrin$_G$ (B and E) demonstrates that NF155 is localized to the paranodes, whereas NF186 is at the node itself (the respective overlays are shown in C and F). Bars: (C and D) 5 μm; (F) 1 μm.

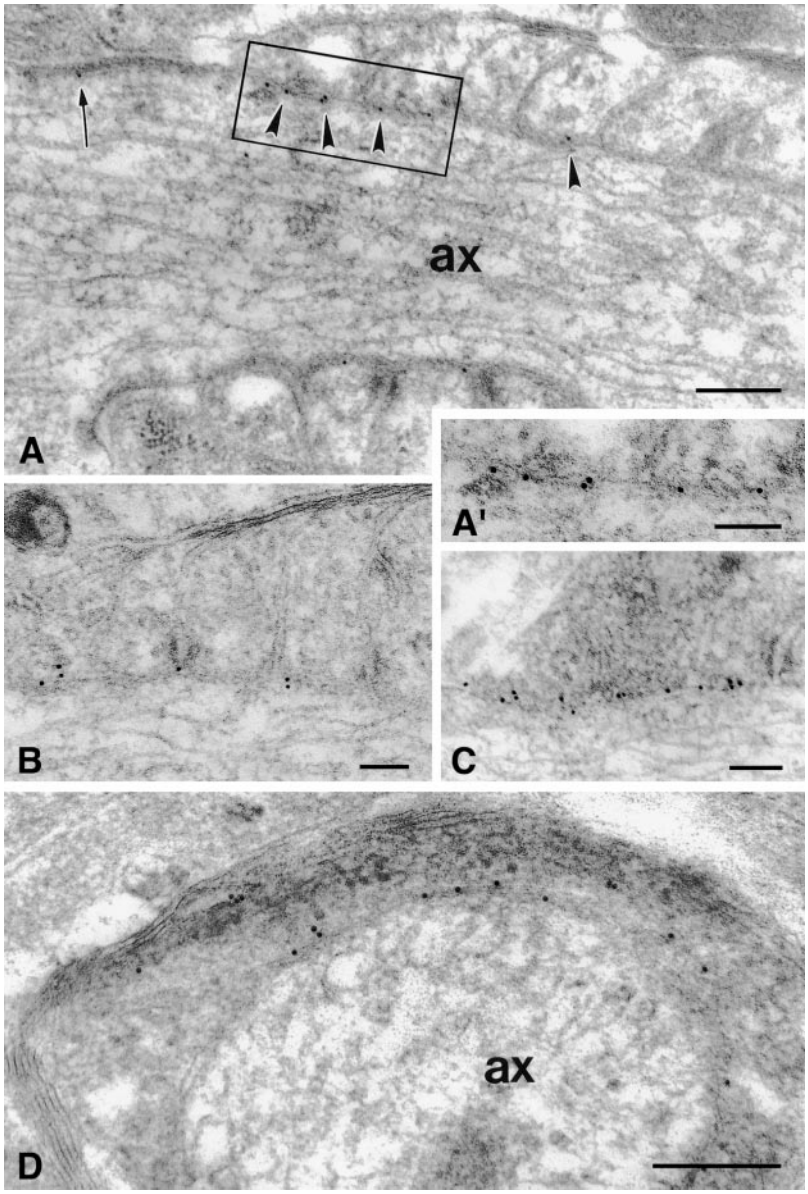

Figure 5. Immunoelectron microscopic detection of NF155 at the paranodal axo-glial junction in mouse optic nerve. (A–C) Immunogold labeling of longitudinal sections of paranodes revealed that the 10-nm gold particles were concentrated at the base of the glial paranodal loops in the axo-glial junction (arrowheads), a single gold particle is observed at the node (arrow) which reflects labeling of NF186. A higher magnification of the boxed area of A is shown in A′. (D) A tangential section of a paranode shows strong labeling at the axon-glial interface. The axon (ax) is indicated. Bars: (A) 200 nm; (A′, B, and C) 100 nm; (D) 200 nm.

lated at P12, a time when it has become restricted to the axo-glial junction (Fig. 6).

NF155 of Myelinating Glia Colocalizes with Neuronal Caspr1/Paranodin at Paranodes

Caspr1/paranodin is known to be an axonal constituent of the paranodal axo-glial junction (Einheber et al., 1997; Menegoz et al., 1997; Peles et al., 1997a,b). Further substantiation of the restriction of NF155 to the paranodal regions of mouse optic nerve axons was provided by its colocalization with Caspr1 (Fig. 7, A and B), which was also observed at the paranodes formed by Schwann cells in mouse sciatic nerve (Fig. 7, C–E). Additionally, in the sciatic nerve, both antibodies decorated a helical ribbonlike structure (Fig. 7 E, arrow), which probably represents the interface between the inner mesaxon of the myelin sheath and the axon. In situ hybridization of the mouse sciatic nerve with an NF155-specific riboprobe demonstrated strong labeling of Schwann cells indicating that, as in the CNS, NF155 was a product of myelin-forming glial cells (Fig. 7 F). NF155 antibodies also stained the cytoplasm-filled channels in the sheath, the Schmidt-Lantermann incisures, where the protein colocalized with MAG (Fig. 7 G), but the apposed axon was not enriched in Caspr1 (data not shown). Immunostaining of cocultures of myelinating rat Schwann cells and dissociated DRG neurons (Fig. 7 H) revealed that the colocalized NF155 and Caspr1 at the paranodes could be resolved into a series of annuli, which probably reflects the lower density of packing of the paranodal loops at the axo-glial junction adhesion zone in this in vitro model of myelination by comparison with intact sciatic nerve fibers (Fig. 7, C and H).

NF155 Is Mislocalized in the Absence of Axo-Glial Junction Formation

The *Shiverer* (*Shi*) mouse lacks the major structural protein myelin basic protein (Roach et al., 1985). *Shi* oligo-

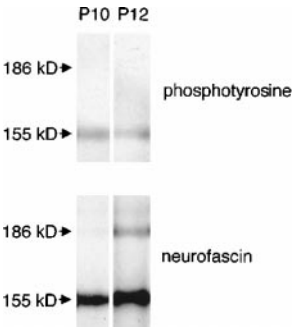

Figure 6. Western blots of NF186 and NF155 immunoprecipitated with the antibody NFC1 from optic nerve homogenates at P10 and P12 probed successively with antibodies to phosphotyrosine and with NFC1, which identifies both isoforms. NF155 is phosphorylated at P12 when it has localized to the axo-glial junction, whereas NF186 was not phosphorylated at P12 when it is first detectable in the optic nerve at the node of Ranvier.

dendrocytes extend processes around axons in the CNS, but they are unable to produce compact myelin, neither do they assemble paranodal axo-glial junctions (Inoue et al., 1981; Rosenbluth, 1981). The absence of paranodes is reflected by the abnormal distribution of Caspr1 (Rasband et al., 1999). Therefore, it was of interest to investigate how this disruption might affect the localization of glial neurofascin. In *Shi* mice, neurofascin displays an immature localization in that the protein is strongly expressed in oligodendrocyte cell bodies (Fig. 8, G and J), and there is no indication that it is targeted to discrete domains that correspond to paranodes, as occurs in the nerves of wild-type littermates where neurofascin and Caspr1 colocalize (Fig. 8, A–F). In spite of their inability to establish a normal axo-glial junction, immunolabeling of *Shi* nerves for Caspr1 revealed that the protein was not distributed diffusely along the axon, but instead was concentrated in discrete patches (Fig. 8, G, J, and M) where it frequently colocalized with NF155 (Fig. 8, I, L and O). This colocalization suggested that Caspr1 and NF155 might still be apposed in the glial and axonal plasma membranes, albeit at an ectopic site. However, the fact that Caspr1 and contactin did not coimmunoprecipitate with NF155 from the brain using either neurofascin or Caspr1 antibodies suggests that Caspr1 and NF155 do not interact directly (data not shown).

Discussion

The sites of interaction between the terminal loops of paranodal myelin and the axon are characterized by a narrow gap of 2.5–3 nm. These junctions represent highly specialized zones that are likely to have a distinctive com-

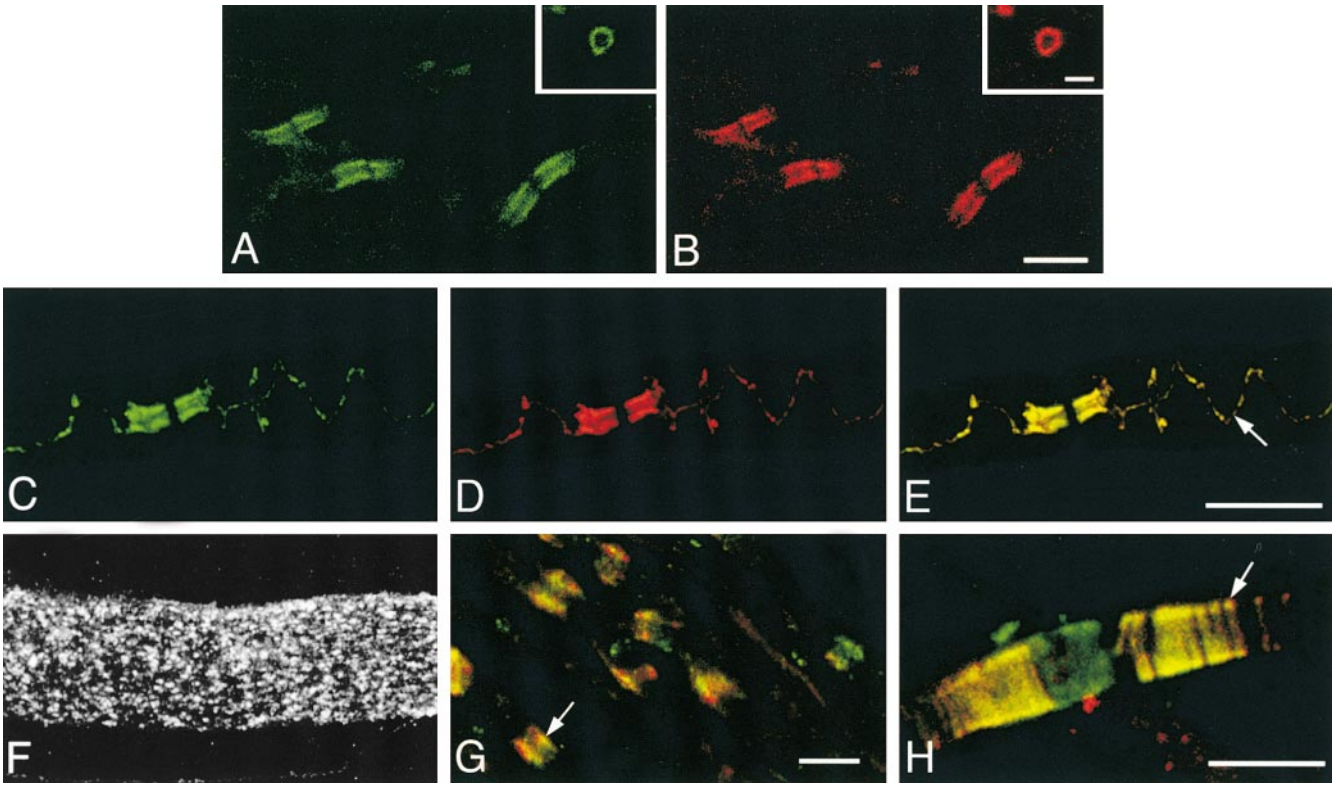

Figure 7. NF155 and Caspr1/paranodin colocalize at the axo-glial junction in the CNS and PNS. NF155 (in green) colocalization with Caspr1 (in red) at the paranodes of mouse optic nerve is shown in a longitudinal section and in a transverse section (A and B, inset). NF155 (green) and Caspr1 (red) also colocalize at the paranodes of teased adult mouse sciatic nerve fibers (C and D). Furthermore, the overlay of the two images (E) reveals a helical ribbon stained by both antibodies, which extends from the paranodal region across the internode in which both proteins are in register (E, arrow). Radioactive in situ hybridization visualized by dark-field microscopy confirmed that NF155 is expressed by Schwann cells in mouse sciatic nerve (F). MAG (red) and NF155 (green) are both constituents of Schmidt-Lantermann incisures (G). A node and paranode in a Schwann cell–DRG neuron coculture are both stained with the NFC1 antibody (green) that recognizes both NF155 and NF186; in contrast, Caspr1 (in red) is restricted to the paranodes (H). Note the annular appearance of the paranodal loops (arrow). Bars: (B, E, and G) 10 μm; (H), 2.5 μm.

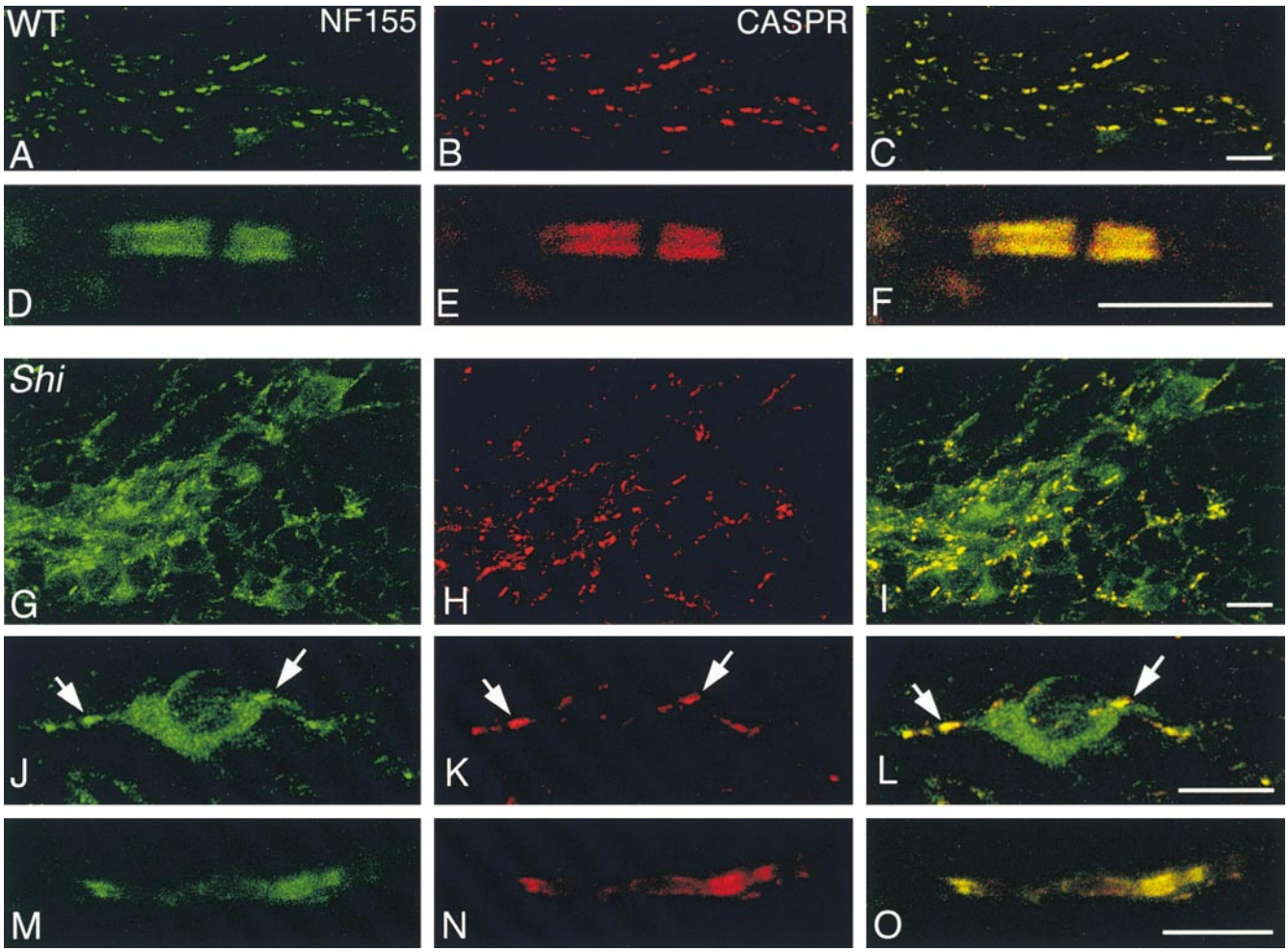

Figure 8. Compared with wild-type mice, NF155 (green) in the cerebellar white matter of *Shiverer* (*Shi*) mice is not targeted to paranodes but colocalizes with Caspr1 (red) at ectopic sites. At P16 in wild-type mice, NF155 (A and D) and Caspr1 (B and E) are localized to paranodes where they colocalize (C and F). In contrast *Shi* oligodendrocytes retain high levels of NF155 (G and J) and do not target the protein to paranodes. Nevertheless, NF155 and Caspr1 are frequently seen to colocalize on fibers at ectopic sites (H and I, K and L, N and O, arrows) that do not have the normal morphological appearance of paranodes (F). Bars: (C, I, and L) 10 μm; (F and O) 5 μm.

plement of adhesion molecules. Furthermore, unlike the tightly compacted lamellae found in the rest of the myelin sheath, the paranodal myelin loops are filled with cytoplasm, which would facilitate the transduction of signals from these transmembrane proteins to the cell body of the myelin-forming glial cell. We have previously shown that the cell adhesion molecule E-cadherin is strongly expressed in these paranodal loops (Fannon et al., 1995). However, E-cadherin does not appear to be a component of the axo-glial junction, but is rather a constituent of adherens junctions at the proximal constrictions of the loops. Another member of the immunoglobulin superfamily, MAG, is also found in the paranodal loops in the PNS and in periaxonal membranes but is not concentrated at the junctional complex (Trapp et al., 1989a,b). Hence, the NF155 isoform of neurofascin is the first glial cell adhesion molecule of the axo-glial junction to be described.

What are the signals that initiate the development of this regional specialization? The axonal transmembrane proteins neurofascin and NrCAM, both members of the L1 cell adhesion molecule family, have been proposed as pioneer molecules in defining the site of node formation (Lambert et al., 1997). We have confirmed previous work that NF186 clusters at the node and is the axonal isoform of neurofascin (Davis et al., 1996). Localization of this isoform to the node of Ranvier is coincident with the first appearance of ankyrin$_G$ in the myelinating optic nerve (data not shown). Hence, it is likely that these proteins play an important role in assembling the molecular machinery required for generating the action potential typical of saltatory nerve impulse conduction at the node as suggested previously by Bennett and co-workers (Davis et al., 1996; Lambert et al., 1997).

It seems likely that physical interaction between the oligodendrocyte and the axon also plays an essential part in defining the site of node assembly. The axo-glial adhesion zone and the invertebrate septate junction both contain members of the NCP (for neurexin IV, Caspr1/paranodin, and Caspr2) subgroup of the neurexin superfamily (Menegoz et al., 1997; Peles et al., 1997a,b; Bellen et al., 1998; Po-

liak et al., 1999). Neurexin IV is a constituent of the pleated septate junctions of *Drosophila* that play an important role in mediating glial–glial interactions (Baumgartner et al., 1996), and Caspr1/paranodin has been shown to be a constituent of paranodal junctions in both the CNS and PNS (Einheber et al., 1997; Menegoz et al., 1997). In the developing optic nerve, it appears that the targeting of Caspr1 to prospective paranodes has a deterministic role (Rasband et al., 1999). Indeed, without correct axon–glial contact, ankyrin$_G$ fails to localize to the node (Rasband et al., 1999). The clustering of sodium channels occurs after the paranodes have been defined and after ankyrin$_G$ and NF186 have codistributed at the node (Rasband et al., 1999; and this work). Hence, one function of the paranodal junctions may be to prevent the diffusion of sodium channels from the nodes, where they are essential participants in the generation of the action potential. The interaction between Caspr1, neurofascin, and their respective ligands would play an important part in ensuring this restricted distribution.

The integrity of the paranodal adhesive junction between axons and myelin-forming glia is not only vital for the establishment of rapid rates of nerve impulse conduction during development, but it is also crucial for the maintenance of normal function in the mature nerve. Subtle derangements in the interactions between the paranodal loops of the myelin sheath and the axon represent the earliest structural correlates of decreased rates of nerve impulse conduction in myelinated fibers and may explain paralysis in some pathologically mild cases of demyelinating disease (Griffin et al., 1996). In support of the importance of the integrity of the axo-glial junction for normal function in myelinated fibers, a mouse mutant, which lacks the enzyme UDP-galactose-ceramide galactosyltransferase (CGT), and which is therefore unable to synthesize the major myelin constituent galactocerebroside, assembles compact myelin but has paranodal myelin loops that do not make structurally normal connections with the axon (Coetzee et al., 1996; Dupree et al., 1998, 1999). Consequently, the conduction properties of the axons are severely compromised, probably as a result of the aberrant exposure of potassium channels in the juxtaparanodal domain of the axonal membrane to the perinodal ionic environment. This conclusion is supported by the positive effect of the potassium channel blocker 4-aminopyridine on the amplitude of nerve impulse conduction in the CNS fibers of CGT mutant mice (Coetzee et al., 1996).

In the myelinating optic nerve, the initiation of axo-glial adhesion assembly is a very early event, since paranodal junctions have been detected as soon as the first spiral of the oligodendrocyte process has ensheathed an axon (Wiggins et al., 1988). Hence, the early targeting of NF155 to the paranodal myelin loops in the optic nerve probably reflects the importance of this protein in the early establishment and stabilization of axon–glial contact. The mechanism by which this targeting is achieved has yet to be determined, but the COOH terminus of the neurofascins does contain a functional ankyrin-binding site that is regulated by tyrosine phosphorylation (Davis et al., 1993; Davis and Bennett, 1994; Garver et al., 1997). Dephosphorylation is required for ankyrin binding, which would suggest that NF155 may only become fully competent to interact with the actin cytoskeleton after it has reached its paranodal destination, since phosphorylation of the protein in the optic nerve is still detectable after it has concentrated at the paranode. This would suggest that the actin cytoskeleton is more likely to be important for neurofascin's function at the paranode rather than in ensuring delivery of this cell adhesion molecule to the axo-glial junction.

The axonal ligand for NF155 has yet to be identified. At first sight, Caspr1 is a strong candidate, particularly in view of the fact that both proteins not only colocalize at normal paranodes, but they also codistribute at ectopic sites in the nerves of *Shi* mutant mice that are unable to assemble paranodes (Rasband et al., 1999). Furthermore, the two proteins codistribute in the PNS, where the inner mesaxon of the myelin sheath apposes the axon. However, these proteins do not colocalize at the Schmidt-Lantermann incisures, which are cytoplasm-filled channels in the compact peripheral myelin sheath, neither do they coimmunoprecipitate from the brain. Hence, it seems likely that, although members of a supramolecular adhesion complex, they are unlikely to interact directly. The other elements of the paranodal axo-glial junction remain to be identified. In view of the importance of this unusual type of mammalian adhesion complex for the cell biology of the neuron, it will be of great interest to further establish its molecular structure. The identification of the glial isoform of neurofascin as a constituent of the junction is a step towards this goal.

We thank Mary Davie (University of Edinburgh) for excellent technical assistance. *Shi* mice were generously supplied by Professor Ian Griffiths (Glasgow University, Glasgow, UK).

The Medical Research Council, the Multiple Sclerosis Society of Great Britain and Northern Ireland, and the Wellcome Trust are thanked for financial support. D.R. Colman is supported by the National Multiple Sclerosis Society and by grants from the National Institutes of Health (NS20147).

Submitted: 9 May 2000
Revised: 13 June 2000
Accepted: 15 June 2000

References

Baumgartner, S., J.T. Littleton, K. Broadie, M.A. Bhat, R. Harbecke, J.A. Lengyel, R. Chiquet-Ehrismann, A. Prokop, and H.J. Bellen. 1996. A *Drosophila* neurexin is required for septate junction and blood-nerve barrier formation and function. *Cell.* 87:1059–1068.

Bellen, H.J., Y. Lu, R. Beckstead, and M.A. Bhat. 1998. Neurexin IV, caspr and paranodin—novel members of the neurexin family: encounters of axons and glia. *Trends Neurosci.* 21:444–449.

Brockes, J.P., K.L. Fields, and M.C. Raff. 1979. Studies in cultured rat Schwann cells. I. Establishment of purified populations from cultures of peripheral nerve. *Brain Res.* 165:105–118.

Brummendorf, T., and F.G. Rathjen. 1996. Structure/function relationships of axon-associated adhesion receptors of the immunoglobulin superfamily. *Curr. Opin. Neurobiol.* 6:584–593.

Brummendorf, T., S. Kenwrick, and F.G. Rathjen. 1998. Neural cell recognition molecule L1: from cell biology to human hereditary brain malformations. *Curr. Opin. Neurobiol.* 8:87–97.

Chiu, S.Y., and J.M. Ritchie. 1981. Evidence for the presence of potassium channels in the paranodal region of acutely demyelinated mammalian single nerve fibres. *J. Physiol.* 313:415–437.

Coetzee, T., N. Fujita, J. Dupree, R. Shi, A. Blight, K. Suzuki, and B. Popko. 1996. Myelination in the absence of galactocerebroside and sulfatide: normal structure with abnormal function and regional instability. *Cell.* 86:209–219.

Collinson, J.M., D. Marshall, C.S. Gillespie, and P.J. Brophy. 1998. Transient expression of neurofascin by oligodendrocytes at the onset of myelinogenesis: implications for mechanisms of axon-glial interaction. *Glia.* 23:11–23.

Davis, J., F. Zhang, Q. Ren, and V. Bennett. 1995. Neurofascin: correlation of

molecular splicing with targeting to nodes of Ranvier and axon initial segments. *Mol. Biol. Cell.* 6:1027–1027.

Davis, J.Q., and V. Bennett. 1994. Ankyrin binding-activity shared by the neurofascin/L1/NrCAM family of nervous-system cell-adhesion molecules. *J. Biol. Chem*. 269:27163–27166.

Davis, J.Q., T. McLaughlin, and V. Bennett. 1993. Ankyrin-binding proteins related to nervous system cell adhesion molecules: candidates to provide transmembrane and intracellular connections in adult brain. *J. Cell Biol.* 121:121–133.

Davis, J.Q., S. Lambert, and V. Bennett. 1996. Molecular composition of the node of Ranvier: identification of ankyrin-binding cell adhesion molecules neurofascin (mucin+ 3rd FNIII domain) and NrCAM at nodal axon segments. *J. Cell Biol.* 135:1355–1367.

Dupree, J.L., T. Coetzee, A. Blight, K. Suzuki, and B. Popko. 1998. Myelin galactolipids are essential for proper node of Ranvier formation in the CNS. *J. Neurosci.* 18:1642–1649.

Dupree, J.L., J.A. Girault, and B. Popko. 1999. Axo-glial interactions regulate the localization of axonal paranodal proteins. *J. Cell Biol.* 147:1145–1151.

Einheber, S., G. Zanazzi, W. Ching, S. Scherer, T.A. Milner, E. Peles, and J.L. Salzer. 1997. The axonal membrane protein Caspr, a homologue of neurexin IV, is a component of the septate-like paranodal junctions that assemble during myelination. *J. Cell Biol.* 139:1495–1506.

Fannon, A.M., D.L. Sherman, G. Ilyina-Gragerova, P.J. Brophy, V.L. Friedrich, and D.R. Colman. 1995. Novel E-cadherin–mediated adhesion in peripheral nerve: Schwann cell architecture is stabilized by autotypic adherens junctions. *J. Cell Biol.* 129:189–202.

Garver, T.D., Q. Ren, S. Tuvia, and V. Bennett. 1997. Tyrosine phosphorylation at a site highly conserved in the L1 family of cell adhesion molecules abolishes ankyrin binding and increases lateral mobility of neurofascin. *J. Cell Biol.* 7:703–714.

Gillespie, C.S., D.L. Sherman, G.E. Blair, and P.J. Brophy. 1994. Periaxin, a novel protein of myelinating Schwann cells with a possible role in axonal ensheathment. *Neuron*. 12:497–508.

Griffin, J.W., C.Y. Li, C. Macko, T.W. Ho, S.T. Hsieh, P. Xue, F.A. Wang, D.R. Cornblath, G.M. McKhann, and A.K. Asbury. 1996. Early nodal changes in the acute motor axonal neuropathy pattern of the Guillain-Barre syndrome. *J. Neurocytol.* 25:33–51.

Grumet, M., V. Mauro, M.P. Burgoon, G.M. Edelman, and B.A. Cunningham. 1991. Structure of a new nervous system glycoprotein, Nr-CAM, and its relationship to subgroups of neural cell adhesion molecules. *J. Cell Biol.* 113: 1399–1412.

Hassel, B., F.G. Rathjen, and H. Volkmer. 1997. Organization of the neurofasin gene and analysis of developmentally regulated alternative splicing. *J. Biol. Chem*. 272:28742–28749.

Inoue, Y., R. Nakamura, K. Mikoshiba, and Y. Tsukada. 1981. Fine-structure of the central myelin sheath in the myelin deficient mutant Shiverer mouse, with special reference to the pattern of myelin formation by oligodendroglia. *Brain Res.* 219:85–94.

Kaplan, M.R., A. Meyer-Franke, S. Lambert, V. Bennett, I.D. Duncan, S.R. Levinson, and B.A. Barres. 1997. Induction of sodium channel clustering by oligodendrocytes. *Nature*. 386:724–728.

Kleitman, N., P.M. Wood, and R.P. Bunge. 1991. Tissue culture methods for the study of myelination. *In* Culturing Nerve Cells. G. Banker and K. Goslin, editors. MIT Press, Cambridge, Massachusetts. 337–371.

Kordeli, E., S. Lambert, and V. Bennett. 1995. Ankyrin(G): a new ankyrin gene with neural-specific isoforms localized at the axonal initial segment and node of Ranvier. *J. Biol. Chem*. 270:2352–2359.

Lambert, S., J.Q. Davis, and V. Bennett. 1997. Morphogenesis of the node of Ranvier: co-clusters of ankyrin and ankyrin-binding integral proteins define early developmental intermediates. *J. Neurosci.* 17:7025–7036.

Menegoz, M., P. Gaspar, M. Le Bert, T. Galvez, F. Burgaya, C. Palfrey, P. Ezan, F. Arnos, and J.A. Girault. 1997. Paranodin, a glycoprotein of neuronal paranodal membranes. *Neuron*. 19:319–331.

Moscoso, L.M., and J.R. Sanes. 1995. Expression of four immunoglobulin superfamily adhesion molecules (L1, Nr-CAM/Bravo, neurofascin/ABGP, and N-CAM) in the developing mouse spinal-cord. *J. Comp. Neurol.* 352:321–334.

Peles, E., K. Joho, G.D. Plowman, and J. Schlessinger. 1997a. Close similarity between *Drosophila* neurexin IV and mammalian Caspr protein suggests a conserved mechanism for cellular interactions. *Cell.* 88:745–746.

Peles, E., M. Nativ, M. Lustig, M. Grumet, J. Schilling, R. Martinez, G.D. Plowman, and J. Schlessinger. 1997b. Identification of a novel contactin-associated transmembrane receptor with multiple domains implicated in protein-protein interactions. *EMBO (Eur. Mol. Biol. Organ.) J.* 16:978–988.

Poliak, S., L. Gollan, R. Martinez, A. Custer, S. Einheber, J.L. Salzer, J.S. Trimmer, P. Shrager, and E. Peles. 1999. Caspr2, a new member of the neurexin superfamily, is localized at the juxtaparanodes of myelinated axons and associates with K^+ channels. *Neuron*. 24:1037–1047.

Rasband, M.N., E. Peles, J.S. Trimmer, S.R. Levinson, S.E. Lux, and P. Shrager. 1999. Dependence of nodal sodium channels clustering on paranodal axoglial contact in the developing CNS. *J. Neurosci.* 19:7516–7528.

Rathjen, F.G., and M. Schachner. 1984. Immunocytological and biochemical characterization of a new neuronal cell-surface component (L1-antigen) which is involved in cell-adhesion. *EMBO (Eur. Mol. Biol. Organ.) J.* 3:1–10.

Rathjen, F.G., J.M. Wolff, S. Chang, F. Bonhoeffer, and J.A. Raper. 1987a. Neurofascin: a novel chick cell-surface glycoprotein involved in neurite-neurite interactions. *Cell*. 51:841–849.

Rathjen, F.G., J.M. Wolff, R. Frank, F. Bonhoeffer, U. Rutishauser, and A. Schoeffski. 1987b. Membrane-glycoproteins involved in neurite fasciculation. *J. Cell Biol.* 104:343–353.

Ritchie, J.M., and R.B. Rogart. 1977. Density of sodium channels in mammalian myelinated nerve fibers and nature of the axonal membrane under the myelinated sheath. *Proc. Natl. Acad. Sci. USA*. 74:211–215.

Roach, A., N. Takahashi, D. Pravtcheva, F. Ruddle, and L. Hood. 1985. Chromosomal mapping of mouse myelin basic protein gene and structure and transcription of the partially deleted gene in shiverer mutant mice. *Cell*. 43: 149–155.

Rosenbluth, J. 1981. Axoglial junctions in the mouse mutant Shiverer. *Brain Res.* 208:283–297.

Salzer, J.L. 1997. Clustering sodium channels at the node of Ranvier: close encounters of the axon-glia kind. *Neuron*. 18:843–846.

Trapp, B.D., S.B. Andrews, C. Cootauco, and R. Quarles. 1989a. The myelin-associated glycoprotein is enriched in multivesicular bodies and periaxonal membranes of actively myelinating oligodendrocytes. *J. Cell Biol.* 109:2417–2426.

Trapp, B.D., S.B. Andrews, A. Wong, M. O'Connell, and J.W. Griffin. 1989b. Co-localization of the myelin-associated glycoprotein and the microfilament components, F-actin and spectrin, in Schwann cells of myelinated nerve fibers. *J. Neurocytol.* 18:47–60.

Tuvia, S., T.D. Garver, and V. Bennett. 1997. The phosphorylation state of the FIGQY tyrosine of neurofascin determines ankyrin-binding activity and patterns of cell segregation. *Proc. Natl. Acad. Sci. USA*. 94:12957–12962.

Vabnick, I., and P. Shrager. 1998. Ion channel redistribution and function during development of the myelinated axon. *J. Neurobiol.* 37:80–96.

Volkmer, H., and F.G. Rathjen. 1992. Variant forms of the chick axon-associated surface glycoprotein neurofascin are differentially expressed during embryonic-development. *Eur. J. Neurosci.* S5:86.

Volkmer, H., B. Hassel, J.M. Wolff, R. Frank, and F.G. Rathjen. 1992. Structure of the axonal surface recognition molecule neurofascin and its relationship to a neural subgroup of the immunoglobulin superfamily. *J. Cell Biol.* 118:149–161.

Wiggins, R.C., G. Chongjie, C. Delaney, and T. Samorajski. 1988. Development of axonal-oligodendrocyte relationships and junctions during myelination of the optic nerve. *Int. J. Dev. Neurosci.* 6:233–243.

Zhang, X., J.Q. Davis, S. Carpenter, and V. Bennett. 1998. Structural requirements for association of neurofascin with ankyrin. *J. Biol. Chem*. 273:30785–30794.